Available online at www.scholarsresearchlibrary.com

Scholars Research Library

Der Pharmacia Lettre, 2013, 5 (2):135-142
(http://scholarsresearchlibrary.com/archive.html)

ISSN 0975-5071
USA CODEN: DPLEB4

Inhibition of carbon steel corrosion in phosphoric acid solution by Alizarin red

D. Ben Hmamou[1], R. Salghi[1], A. Zarrouk[2,*], H. Zarrok[3], M. Assouag[3], B. Hammouti[2], S. S. Al-Deyab[4] and M. El Hezzat[5]

[1]*Laboratory of Environmental Engineering and Biotechnology, ENSA, University Ibn Zohr, PO Box 1136, 80000 Agadir, Morocco*
[2]*LCAE-URAC 18, Faculty of Science, University of Mohammed Premier, Po Box 717 60000 Oujda, Morocco*
[3]*Laboratory separation processes, Faculty of Science, University Ibn Tofail PO Box 242, Kenitra, Morocco*
[4]*Petrochemical Research Chair, Chemistry Department, College of Science, King Saud University, P.O. Box 2455, Riyadh 11451, Saudi Arabia*
[5]*Laboratoire de Physico-Chimie du Solide (LPCS), Faculté des Sciences, Université Ibn Tofail, B.P. 133, 14000 Kenitra, Morocco*

ABSTRACT

The inhibition effect of alizarin red (AZR) on the corrosion of carbon steel in 2.0 M H_3PO_4 solutions at 298K was investigated by using electrochemical impedance spectroscopy EIS, potentiodynamic polarization and weight loss measurements. A significant decrease in the corrosion rate of steel was observed in the presence of investigated alizarin red. Potentiodynamic polarization curves revealed that this inhibitor acted as mixed-type inhibitor, affecting both cathodic and anodic corrosion processes. The adsorption of the inhibitor on carbon steel surface in 2.0 M H_3PO_4 was found to follow Langmuir adsorption isotherm. Thermodynamic adsorption parameters (K, ΔG°_{ads}) of investigated inhibitor were calculated from the linear form of Langmuir adsorption isotherm.

Keywords: Alizarin red, Corrosion, Carbon steel, EIS, Polarization, Weight loss.

INTRODUCTION

Carbon steel as an important construction material is extensively used in all kinds of industry and corrosion of carbon steel known to occur especially in acid environment such as cleaning, pickling, oil well acidification and descaling processes [1-5]. It is a major task to control the carbon steel corrosion for both corrosion scientist and material technologist. Several methods are employed to prevent carbon steel from corrosion but addition of inhibitors has been known to be the most effective method for its practical application [6-9]. A large number of studies about various types of organic inhibitors have been previously reported [10-32]. Organic molecules can form a barrier through adsorption on the metal surface to reduce the corrosion of metal in acidic solution [33]. So most of efficient inhibitors are organic compounds in their structures containing heteroatoms (such as, N, S, and O) donating lone pair electrons, unsaturated bonds (such as double bonds, or triple bonds), and plane conjugated systems including all kinds of aromatic cycles [34-37]. Furthermore, organic inhibitor adsorption on metal surface is influenced by organic inhibitor nature, surface charges on the metal, the type of aggressive solution, and the interaction of inhibitor with the metal surface.

Phosphoric acid shows strong corrosiveness on ferrous and ferrous alloys. There is a great need to protect steel materials used in the phosphoric acid industry. However, several works [38-44] appears to have been done on the corrosion inhibition of steel in phosphoric acid solutions. Khamis et al. [43] investigated the corrosion inhibition of steel in 35% H_3PO_4 by some thiosemicarbazide derivatives. Their results showed that the protection efficiency of all

the compounds reached up to 99%. However, it has been reported [45] that the inhibitors which are useful in hydrochloric acid solutions are generally also effective in H_3PO_4 solutions.

The goal of this work is to study the effectiveness and electrochemical behavior of alizarin red on the corrosion behavior of the carbon steel in 2.0 M H_3PO_4 solution by using standard electrochemical techniques as polarization curves, electrochemical impedance spectroscopy (EIS), and weight loss measurements. The structure of the alizarin red that used in this study can be shown below:

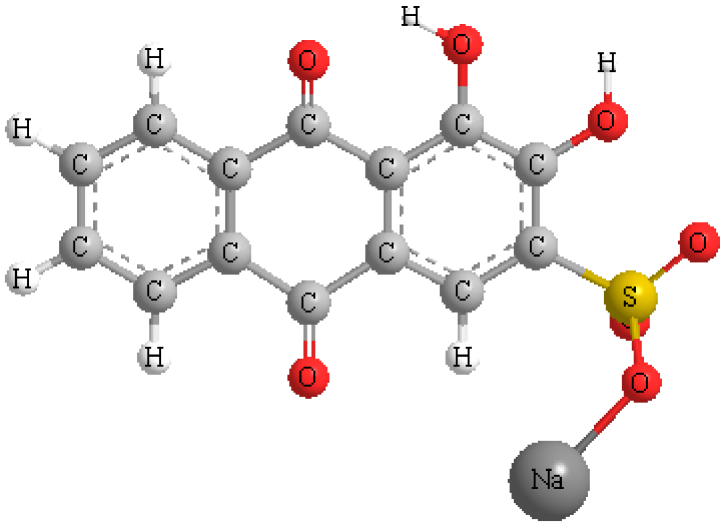

Figure 1. The molecular structure of alizarin red.

MATERIALS AND METHODS

Materials

The steel used in this study is carbon steel (Euronorm: C35E carbon steel and US specification: SAE 1035) with a chemical composition (in wt%) of 0.370 % C, 0.230 % Si, 0.680 % Mn, 0.016 % S, 0.077 % Cr, 0.011 % Ti, 0.059 % Ni, 0.009 % Co, 0.160 % Cu and the remainder iron (Fe). The carbon steel samples were pre-treated prior to the experiments by grinding with emery paper SiC (120, 600 and 1200); rinsed with distilled water, degreased in acetone in an ultrasonic bath immersion for 5 min, washed again with bidistilled water and then dried at room temperature before use. The acids solution (2.0 M H_3PO_4) was prepared by dilution of an analytical reagent grade 85% H_3PO_4 with double-distilled water. The concentration range of AZR employed was 10^{-5} M to 10^{-2} M.

Measurements

Weight loss measurements

Gravimetric measurements were carried out at definite time interval of 2 h at room temperature using an analytical balance (precision ± 0.1 mg). The carbon steel specimens used have a rectangular form (length = 1.6 cm, width = 1.6 cm, thickness = 0.07 cm). Gravimetric experiments were carried out in a double glass cell equipped with a thermostated cooling condenser containing 80 mL of non-de-aerated test solution. After immersion period, the steel specimens were withdrawn, carefully rinsed with bidistilled water, ultrasonic cleaning in acetone, dried at room temperature and then weighted. Triplicate experiments were performed in each case and the mean value of the weight loss was calculated.

Electrochemical measurements

Electrochemical experiments were conducted using impedance equipment (Tacussel-Radiometer PGZ 100) and controlled with Tacussel corrosion analysis software model Voltamaster 4. A conventional three-electrode cylindrical Pyrex glass cell was used. The temperature was thermostatically controlled. The working electrode was carbon steel with the surface area of 1 cm^2. A saturated calomel electrode (SCE) was used as a reference. All potentials were given with reference to this electrode. The counter electrode was a platinum plate of surface area of 1 cm^2. A saturated calomel electrode (SCE) was used as the reference; a platinum electrode was used as the counter-electrode. All potentials are reported *vs*. SCE. All electrochemical tests have been performed in aerated solutions at 298 K.

For polarization curves, the working electrode was immersed in a test solution during 30 min until a steady state open circuit potential (E_{ocp}) was obtained. The polarization curve was recorded from -800 to -200 mV/SCE with a scan rate of 1 mV s^{-1}. AC impedance measurements were carried-out in the frequency range of 100 kHz to 10 mHz,

with 10 points per decade, at the rest potential, after 30 min of acid immersion, by applying 10 mV ac voltage peak-to-peak. Nyquist plots were made from these experiments. The best semicircle was fit through the data points in the Nyquist plot using a non-linear least square fit so as to give the intersections with the *x*-axis.

RESULTS AND DISCUSSION

Tafel polarization

The anodic and cathodic polarization behavior of carbon steel in 2.0 M H_3PO_4 in the absence and presence of different concentrations of AZR is given in Fig. 2. The extrapolation method for the polarization curves was applied and the data for corrosion potential (E_{corr}), corrosion current density (I_{corr}), and Tafel slopes (b_c) are shown in Table 1. The results in Fig. 2 and Table 1 illustrate that as the additive concentration increases there is a shift in the corrosion current density (I_{corr}) to lower values relative to the blank. Meanwhile, the corrosion potential (E_{corr}) is shifted to the noble direction values. The results indicate that the additives provide an inhibition effect on the corrosion of carbon steel electrodes in 2.0 M H_3PO_4 solutions and behave mainly as a mixed-type inhibitor. The values of I_{corr} decreases with increasing inhibitor concentration and the Tafel slopes remain almost unchanged, indicating that the presence of these compound in the solution has no effect on the mechanism of the dissolution process of the metal and the adsorbed molecules mechanically screen the coated part of the electrode and therefore protect it from the action of the corrosion medium [46, 47].

The reaction mechanism of the corrosion process in 2.0 M H_3PO_4 solution free from inhibitor is different from that in the presence of the inhibitor. From the inspection of data given in Table 1, it is clear that in the presence of inhibitor the value of b_c is greater than that in free acid solution. This behavior could be due to the decrease of the cathodic transfer coefficient, which can be ascribed to the thickening of the electric double layer or the formation of multimolecular layers on the metal surface [48]. The percentage inhibition efficiency, η_{Tafel} (%), was calculated using the following equation and is listed in Table 1:

$$\eta_{Tafel}\% = \frac{I^{\circ}_{corr} - I^{i}_{corr}}{I^{\circ}_{corr}} \times 100 \qquad (1)$$

where, I°_{corr} and I^{i}_{corr} are the corrosion current density in absence and presence of inhibitor, respectively. The corrosion current densities are calculated from the intersections of the cathodic curves with stationary corrosion potentials (E_{corr}). The obtained η_{Tafel} (%) values (Table 1) reveal that the order of inhibition efficiency increases with increasing inhibitor concentration.

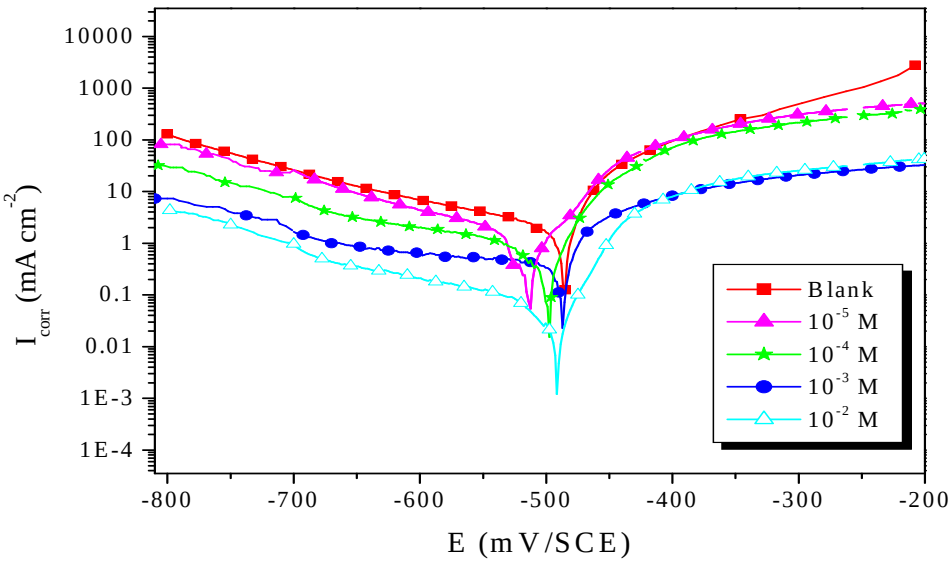

Figure 2. Potentiodynamic polarisation curves of carbon steel in 2.0 M H_3PO_4 in the presence of different concentrations of AZR.

Table 1. Electrochemical parameters of carbon steel at various concentrations of AZR in 2.0 M H_3PO_4 and corresponding inhibition efficiency.

Inhibitor	Conc (M)	E_{corr} (mV/SCE)	I_{corr} ($\mu A/cm^2$)	$-b_c$ (mV/dec)	η_{Tafel} (%)
Blank	2.00	-506	2718	135	-----
AZR	10^{-2}	-492	173	145	93.6
	10^{-3}	-488	473	132	82.6
	10^{-4}	-499	950	146	65.0
	10^{-5}	-513	1240	143	54.4

Electrochemical impedance spectroscopy measurements

Impedance diagrams (Nyquist) at frequencies ranging from 100 kHz to 10 mHz with 10 mV amplitude signal at OCP for carbon steel in 2.0 M H_3PO_4 in the absence and presence of different concentrations of this compound are obtained. The equivalent circuit that describes our metal/electrolyte interface is shown in Fig. 3 where R_s, R_{ct} and CPE refer to solution resistance, charge transfer resistance and constant phase element, respectively.

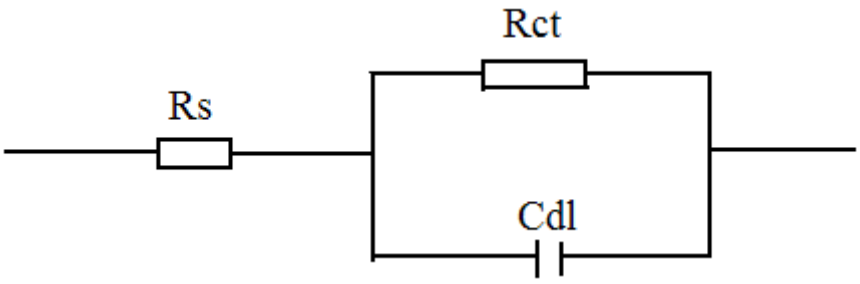

Figure 3. Equivalent circuit of constant phase element (CPE).

EIS parameters and % η_i were calculated and tabulated in Table 2.

Table 2. Electrochemical Impedance parameters for corrosion of steel in acid medium at various contents of AZR.

Inhibitor	Conc (M)	R_{ct} ($\Omega\ cm^2$)	f_{max} (Hz)	C_{dl} ($\mu F\ cm^{-2}$)	η_i (%)
Blank	2.00	20.68	148.50	51.82	-----
AZR	10^{-2}	160.00	63.15	15.75	87.1
	10^{-3}	90.26	97.32	18.11	77.0
	10^{-4}	57.20	134.40	20.70	63.7
	10^{-5}	40.60	156.20	25.09	48.3

The obtained Nyquist plot for this compound is shown in Fig. 4. Each spectrum is characterized by a single full semicircle. The fact that impedance diagrams have an approximately semicircular appearance shows that the corrosion of carbon steel is controlled by a charge transfer process. The diameters of the capacitive loop obtained increases in the presence of AZR, and were indicative of the degree of inhibition of the corrosion process. It was observed from the obtained EIS data that R_{ct} increases and C_{dl} decreases with the increasing of inhibitor concentrations. The increase in R_{ct} values, and consequently of inhibition efficiency, may be due to the gradual replacement of water molecules by the adsorption of the inhibitor molecules on the metal surface to form an adherent film on the metal surface and this suggests that the coverage of the metal surface by the film decreases the double layer thickness. Also, this decrease of C_{dl} at the metal/solution interface with increasing the inhibitor concentration can result from a decrease in local dielectric constant which indicates that the inhibitor was adsorbed on the surface at both anodic and cathodic sites [49]. The impedance data confirm the inhibition behavior of the inhibitor obtained with other technique. From the impedance data (Table 2), we conclude that the value of R_{ct} increases with increase in concentration of the inhibitor and this indicates an increase in the corrosion inhibition efficiency, which is in concord with the potentiodynamic polarisation results obtained. In acidic solution, the impedance diagrams show perfect semi-circles (Fig. 4) whose size increases with the concentration of the inhibitor indicating a charge-transfer process mainly controlling the corrosion of steel. In fact, the presence of inhibitor enhances the value of the transfer resistance in acidic solution. Values of double layer capacitance are also brought down to the maximum extent in the presence of inhibitor and decrease in the values of C_{dl}. The decrease in C_{dl} is due to the adsorption of this compound on the metal surface leading to the formation of a film from the acidic solution [50].

Values of the double layer capacitance (C_{dl}) were calculated from the frequency at which the impedance imaginary component ($-Z_{im}$) was maximum, using the following equation:

$$f\left(-Z_{im}\right)=\frac{1}{2\pi C_{dl}R_{ct}} \tag{2}$$

% η_i was calculated using the equation:

$$\eta_i=\left(\frac{R_{ct(inh)}-R_{ct(uninh)}}{R_{ct(inh)}}\right)\times 100 \tag{3}$$

where $R_{ct(inh)}$ and $R_{ct(uninh)}$ are the charge-transfer resistance values with and without inhibitor, respectively.

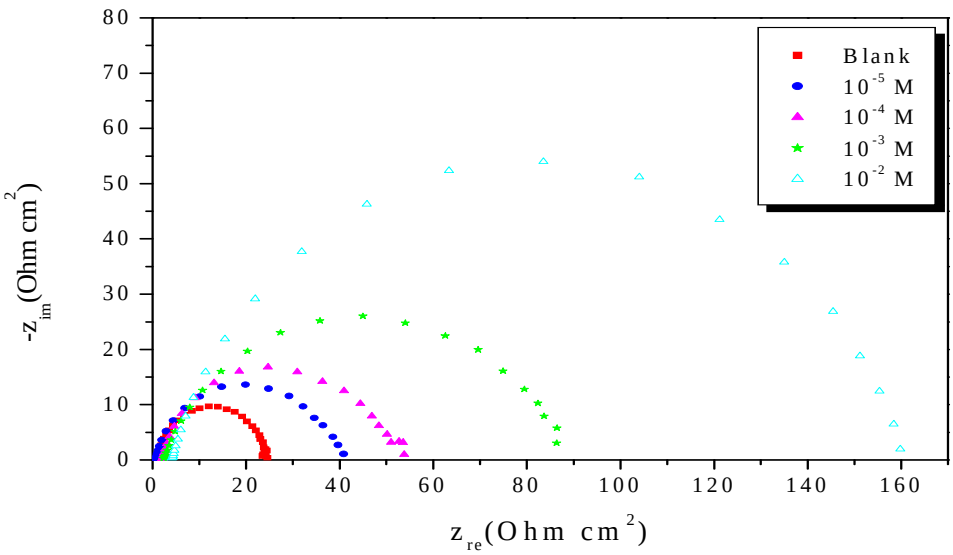

Figure 4. Nyquist diagrams for carbon steel electrode with and without AZR at E_{corr} after 30 min of immersion.

Weight loss, corrosion rates and inhibition efficiency

The corrosion of carbon steel in 2.0 M H_3PO_4 in the absence and presence of various concentrations (10^{-5} to 10^{-2} M) of alizarin red was studied by weight loss experiments. The corrosion rate (υ) and the percentage protection efficiency η_{WL} % were calculated according to the following equations:

$$\upsilon=\frac{w}{St} \tag{3}$$

Where υ was the corrosion rate in (mg cm^{-2} h^{-1}), *w* is the average weight loss of three parallel carbon steel sheets (mg), *S* was the total area of one carbon steel sheet (cm^2), and *t* was immersion time (h).

$$\eta_{WL}\%=\frac{\upsilon_0-\upsilon}{\upsilon_0}\times 100 \tag{4}$$

Where υ_0 and υ are the values of corrosion rate without and with different concentration of inhibitor, respectively.

The values of inhibition efficiencies and corrosion rates obtained from gravimetric measurements with the addition of different concentrations of AZR after 2 h immersion in 2.0 M H_3PO_4 solutions at 298K are summarized in Table 3. The addition of this compound inhibits the acid corrosion of steel at all concentrations used in this study. The inhibition efficiency increases with the increase in concentration. The optimum concentration for maximum efficiency was found to be 10^{-2} M. At the optimum concentration, the efficiency attains 90.0 % at 298K. The corrosion inhibition can be attributed to the adsorption of the inhibitor at the steel/acid solution interface. The ability of the molecule to chemisorb on the steel surface was dependent on the heteroatoms and the electron density on these atoms [51]. The high inhibitive efficiency is due to the bonding of (adsorbed) AZR onto the metal surface; the

strong bonding is mainly attributed to higher electron densities at active functional groups present in the adsorbate molecule.

Table 3. Effect of AZR concentration on corrosion data of steel in 2.0 M H_3PO_4.

Inhibitor	Conc (M)	υ (mg cm^{-2} h^{-1})	η_{WL} (%)	θ
Blank	2.0	1.972	----	----
AZR	10^{-2}	0.197	90.0	0.900
	10^{-3}	0.387	80.3	0.803
	10^{-4}	0.590	70.0	0.700
	10^{-5}	0.923	53.2	0.532

Adsorption isotherm

Figure 5 shows a plot of C/θ against C for the inhibitor at 298K in H_3PO_4 medium, which gives straight lines with almost unit slope indicating that the inhibitor obeys the Langmuir adsorption isotherm. According to this isotherm θ is related to concentration of inhibitor C via

$$\frac{\theta}{1-\theta} = KC \tag{5}$$

where K is the equilibrium constant of the adsorption process. The values of surface coverage θ were evaluated by mass loss measurements using the equation:

$$\theta = \frac{\upsilon_0 - \upsilon}{\upsilon_0} \tag{6}$$

A linear relationship is obtained with slope equal to K which is related to the standard free energy of adsorption (ΔG°_{ads}) by the equation:

$$K = \frac{1}{55.5}\exp\left(\frac{-\Delta G^{\circ}_{ads}}{RT}\right) \tag{7}$$

where R is gas constant and T is absolute temperature of experiment and the constant value of 55.5 is the concentration of water in solution in mol L^{-1}.

The thermodynamic parameters for the adsorption process were obtained from this figure are shown in Table 4.

Table 4. Thermodynamic parameters for the adsorption of AZR in 2.0 H_3PO_4 on the carbon steel at 298K.

Inhibitor	K (M^{-1})	R^2	ΔG°_{ads} (kJ/mol)
AZR	17523.57	0.99994	-34.16

The value of ΔG°_{ads} is negative which indicate that these investigated compound is strongly adsorbed on the carbon steel surface and show the spontaneity of the adsorption process and stability of the adsorbed layer on the carbon steel surface. Generally, values of ΔG°_{ads} up to -20 kJ mol^{-1} are consistent with the electrostatic interaction between the charged molecules and the charged metal (physical adsorption) while those more negative than -40 kJ mol^{-1} involve sharing or transfer of electrons from the inhibitor molecules to the metal surface to form a coordinate type of bond (chemisorption) [52]. The value of ΔG°_{ads} obtained was approximately equal to -34 kJ mol^{-1}, indicating that the adsorption mechanism of the AZR on carbon steel in 2.0 H_3PO_4 solution involves both electrostatic adsorption and chemisorptions [53]. The large value of K imply better more efficient adsorption and hence better inhibition efficiency [54].

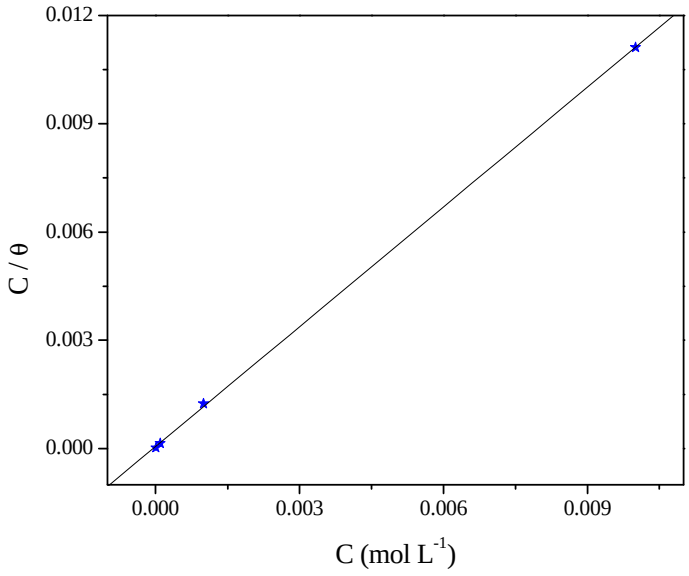

Figure 5. Langmuir adsorption of AZR on the carbon steel surface in 2.0 H_3PO_4 solution.

CONCLUSION

On the basis of the collected data, the following conclusions may be drawn:

- AZR could acts as an effective corrosion inhibitor for the phosphoric acid corrosion of carbon steel.
- AZR is classified as a mixed-type inhibitor with predominant anodic character.
- The decrease in C_{dl} values, obtained from impedance measurements, was related to the decrease of local dielectric constant (ε) or increase of thickness of electrical double layer due to the formation of a protective layer by the adsorption of inhibitor molecules on the carbon steel surface.
- The adsorption of AZR on the surface of steel obeys the Langmuir adsorption isotherm.

REFERENCES

[1] D. M. Strickland, *Ind. Eng. Chem*. **1923**, 15, 566.
[2] J. D. Hatfield, A.V. Slack, G. L. Crow, H. B. Shaffer Jr., *J. Agric. Food. Chem*. **1958**, 6, 524.
[3] W. Guo, S. Chen, Y. Feng, C. Yang, *J. Phys. Chem*. C **2007**, 111, 3109.
[4] S. Lyon, *Nature* **2004**, 427, 406.
[5] I.R. Glasgow, A. J. Rostron, G. Thomson, *Corros. Sci*. **1966**, 6, 469.
[6] N.O. Eddy, E.E. Ebenso, Afr. J. Pure Appl. Chem. **2008**, 2, 1.
[7] A.F. Gualdrón, E.N. Becerra, D.Y. Peña, J.C. Gutiérrez, H.Q. Becerra, *J. Mater. Environ. Sci*. **2013**, 4, 143.
[8] M. Ramananda Singh, *J. Mater. Environ. Sci*. **2013**, 4, 117.
[9] I. B. Obot, S. A. Umoren, N. O. Obi-Egbedi, *J. Mater. Environ. Sci.* **2011**, 2, 49.
[10] A. Ghazoui, N. Bencaht, S. S. Al-Deyab, A. Zarrouk, B. Hammouti, M. Ramdani, M. Guenbour, *Int. J. Electrochem. Sci*. **2013**, 8, 2272.
[11] A. H. Al Hamzi, H. Zarrok, A. Zarrouk, R. Salghi, B. Hammouti, S. S. Al-Deyab, M. Bouachrine, A. Amine, F. Guenoun, *Int. J. Electrochem. Sci*. **2013**, 8, 2586.
[12] H. Zarrok, A. Zarrouk, R. Salghi, H. Oudda, B. Hammouti, M. Assouag, M. Taleb, M. Ebn Touhami, M. Bouachrine and S. Boukhris, *J. Chem. Pharm. Res*. **2012**, 4, 5056.
[13] H. Zarrok, A. Zarrouk, R. Salghi, Y. Ramli, B. Hammouti, M. Assouag, E. M. Essassi, H. Oudda and M. Taleb, *J. Chem. Pharm. Res*. **2012**, 4, 5048.
[14] A. Zarrouk, H. Zarrok, R. Salghi, B. Hammouti, F. Bentiss , R. Touir, M. Bouachrine, *J. Mater. Environ. Sci.* **2013**, 4, 177.
[15] A. Zarrouk, H. Zarrok, R. Salghi, N. Bouroumane, B. Hammouti, S. S. Al-Deyab, R. Touzani, *Int. J. Electrochem. Sci.* **2012**, 7, 10215.
[16]D. Ben Hmamou, R. Salghi, A. Zarrouk, H. Zarrok, S. S. Al-Deyab, O. Benali, B. Hammouti, *Int. J. Electrochem. Sci*. **2012**, 7, 8988.

[17] A. Zarrouk, M. Messali, M. R. Aouad, M. Assouag, H. Zarrok, R. Salghi, B. Hammouti, A. Chetouani, *J. Chem. Pharm. Res*. **2012**, 4, 3427.
[18] M. Elbakri, R. Touir, M. Ebn Touhami, A. Zarrouk, Y. Aouine, M. Sfaira, M. Bouachrine, A. Alami, A. El Hallaoui, *Res. Chem. Intermed*. **2012** DOI: 10.1007/s11164-012-0768-6.
[19] H. Zarrok, A. Zarrouk, R. Salghi, Y. Ramli, B. Hammouti, S. S. Al-Deyab, E. M. Essassi, H. Oudda, *Int. J. Electrochem. Sci*. **2012**, 7, 8958.
[20] H. Bendaha, A. Zarrouk, A. Aouniti, B. Hammouti, S. El Kadiri, R. Salghi, R. Touzani, *Phys. Chem. News*, **2012**, 64, 95.
[21] H. Zarrok, K. Al Mamari, A. Zarrouk, R. Salghi, B. Hammouti, S. S. Al-Deyab, E. M. Essassi, F. Bentiss, H. Oudda, *Int. J. Electrochem. Sci*. **2012**, 7, 10338.
[22] A. Ghazoui, R. Saddik, B. Hammouti, A. Zarrouk, N. Benchat, M. Guenbour, S. S. Al-Deyab, I. Warad, *Res. Chem. Intermed*. **2012** DOI: 10.1007/s11164-012-0763-y.
[23] A. Zarrouk, M. Messali, H. Zarrok, R. Salghi, A. Al-Sheikh Ali, B. Hammouti, S. S. Al-Deyab, F. Bentiss, *Int. J. Electrochem. Sci***. 2012**, 7, 8958.
[24] A. Ghazoui, R. Saddik, N. Benchat, M. Guenbour, B. Hammouti, S.S. Al-Deyab, A. Zarrouk, *Int. J. Electrochem. Sci*. **2012**, 7, 7080.
[25] D. Ben Hmamou, R. Salghi, A. Zarrouk, M. Messali, H. Zarrok, M. Errami, B. Hammouti, Lh. Bazzi , A. Chakir, *Der Pharm. Chem*. **2012**, 4, 1496.
[26] D. Ben Hmamou, R. Salghi, A. Zarrouk, H. Zarrok, B. Hammouti, S. S. Al-Deyab, M. Bouachrine, A. Chakir, M. Zougagh, *Int. J. Electrochem. Sci***. 2012**, 7, 5716.
[27] H. Zarrok, S. S. Al-Deyab, A. Zarrouk, R. Salghi, B. Hammouti, H. Oudda, M. Bouachrine, F. Bentiss, *Int. J. Electrochem. Sci*. **2012**, 7, 4047.
[28] S. Rekkab, H. Zarrok, R. Salghi, A. Zarrouk, Lh. Bazzi, B. Hammouti, Z. Kabouche, R. Touzani, M. Zougagh, *J. Mater. Environ. Sci*. **2012**, 3, 613.
[29] H. Zarrok, H. Oudda, A. El Midaoui, A. Zarrouk, B. Hammouti, M. Ebn Touhami, A. Attayibat, S. Radi, R. Touzani, *Res. Chem. Intermed*. **2012** DOI: 10.1007/s11164-012-0525-x.
[30] H. Zarrok, R. Salghi, A. Zarrouk, B. Hammouti, H. Oudda, Lh. Bazzi, L. Bammou, S. S. Al-Deyab, *Der Pharm. Chem*. **2012**, 4, 407.
[31] A. Ghazoui, R. Saddik, N. Benchat, B. Hammouti, M. Guenbour, A. Zarrouk, M. Ramdani, *Der Pharm. Chem*. **2012**, 4, 352.
[32] H. Zarrok, R. Saddik, H. Oudda, B. Hammouti, A. El Midaoui, A. Zarrouk, N. Benchat, M. Ebn Touhami, *Der Pharm. Chem*. **2011**, 3, 272.
[33]A. Zarrouk, H. Zarrok, R. Salghi, B. Hammouti, F. Bentiss, R. Touir, M. Bouachrine, *J. Mater. Environ. Sci*. **2013**, 4, 177.
[34] H. Zarrok, A. Zarrouk, B. Hammouti, R. Salghi, C. Jama, F. Bentiss, *Corros. Sci*. **2012**, 64, 243.
[35] A .Zarrouk, B. Hammouti, A. Dafali and Fouad Bentiss, *Ind. Eng. Chem. Res.* **2013**, 52, 2560.
[36] A. Zarrouk, A. Dafali, B. Hammouti, H. Zarrok, S. Boukhris, M. Zertoubi, *Int. J. Electrochem. Sci.* **2010**, 5, 46.
[37] A. Zarrouk, T. Chelfi, A. Dafali, B. Hammouti, S.S. Al-Deyab, I. Warad, N. Benchat, M. Zertoubi, *Int. J. Electrochem. Sci.* **2010**, 5, 696.
[38] X. Li, Sh. Deng, H. Fu, *Corros. Sci.* **2011**, 53, 664 .
[39] X. Li, Sh. Deng, H. Fu, Guannan Mu, *Corros. Sci.* **2010**, 52, 1167 .
[40] X. Li, Sh. Deng, H. Fu, *Prog. Org. Coat*. **2010**, 67, 420.
[41] A.Ghanbari, M.M. Attar, M. Mahdavian, *Mater. Chem. Phys*. **2010**, 124, 1205.
[42] E.A. Noor., *Corros. Sci*. **2005**, 47, 33.
[43] E. Khamis, M.A. Ameer, N.M. AlAndis, G. Al-Senani, *Corrosion* **2000**, 56, 127.
[44] M.S. Morad, *Mater. Chem. Phys*. **1999**, 60, 188.
[45] G. Schmitt, *Br. Corros. J*. **1984**, 19, 165.
[46] M.B. Abou El-Khir, I.A. Abdel Hamid, *Corros. Sci*. **1976**, 16, 169.
[47] S. Sankarapavinasam, F. Pushpanaden, M.F. Ahmed, *Corros. Sci*. **1991**, 32, 193.
[48] G. Moretti, G. Quartarane, A. Tassan, A. Zingales, *Electrochim. Acta* **1996**, 41, 1971.
[49] E. McCafferty, N. Hackerman, J. Electrochem. Soc. **1972**, 119, 146.
[50] F. Bentiss, M. Largrenee, M. Traisenl, J.C. Hornez, Corros. Sci. **1999**, 41, 789.
[51] F. Bentiss, M. Lebrini, M. Lagrenee, *Corros. Sci*. **2005**, 47, 2915.
[52] F. Bensajjay, S. Alehyen, M. S. El-Achouri, Kertit, *Anti-Corros. Methods Mater*. **2003**, 50, 402
[53] S.Z. Duan, Y.L. Tao, Interface chemistry. Higher EducationPress, Beijing, **1990**, 124 pp.
[54] S.S. Abd El-Rehim, S.A.M. Refaey, F. Taha, M.B. Saleh, R.A. Ahmed, *J. Appl. Electrochem*. **2001**, 31, 429.